

A Self-restricted CD38-connexin 43 Cross-talk Affects NAD⁺ and Cyclic ADP-ribose Metabolism and Regulates Intracellular Calcium in 3T3 Fibroblasts*

Received for publication, August 1, 2001, and in revised form, October 1, 2001
Published, JBC Papers in Press, October 15, 2001, DOI 10.1074/jbc.M107308200

Santina Bruzzone^{‡§}, Luisa Franco^{§¶}, Lucrezia Guida[‡], Elena Zocchi[‡], Paola Contini^{||},
Angela Bisso[‡], Cesare Usai^{**}, and Antonio De Flora^{‡ §§}

From the [‡]Department of Experimental Medicine, Section of Biochemistry, University of Genova, Viale Benedetto XV/1, Genova, Italy, the [¶]G. Gaslini Institute, Largo G. Gaslini 5, Genova, Italy, the ^{||}Department of Internal Medicine, University of Genova, Viale Benedetto XV/6, Genova, Italy, and the ^{**}Institute of Cybernetics and Biophysics, CNR, Via De Marini, 6 Genova, Italy

Connexin 43 (Cx43) hexameric hemichannels, recently demonstrated to mediate NAD⁺ transport, functionally interact in the plasma membrane of several cells with the ectoenzyme CD38 that converts NAD⁺ to the universal calcium mobilizer cyclic ADP-ribose (cADPR). Here we demonstrate that functional uncoupling between CD38 and Cx43 in CD38-transfected 3T3 murine fibroblasts is paralleled by decreased [Ca²⁺]_i levels as a result of reduced intracellular conversion of NAD⁺ to cADPR. A sharp inverse correlation emerged between [Ca²⁺]_i levels and NAD⁺ transport (measured as influx into cells and as efflux therefrom), both in the CD38⁺ cells (high [Ca²⁺]_i, low transport) and in the CD38[−] fibroblasts (low [Ca²⁺]_i, high transport). These differences were correlated with distinctive extents of Cx43 phosphorylation in the two cell populations, a lower phosphorylation with high NAD⁺ transport (CD38[−] cells) and vice versa (CD38⁺ cells). Conversion of NAD⁺-permeable Cx43 to the phosphorylated, NAD⁺-impermeable form occurs via Ca²⁺-stimulated protein kinase C (PKC). Thus, a self-regulatory loop emerged in CD38⁺ fibroblasts whereby high [Ca²⁺]_i restricts further Ca²⁺ mobilization by cADPR via PKC-mediated disruption of the Cx43-CD38 cross-talk. This mechanism may avoid: (i) leakage of NAD⁺ from cells; (ii) depletion of intracellular NAD⁺ by CD38; (iii) overproduction of intracellular cADPR resulting in potentially cytotoxic [Ca²⁺]_i.

CD38, a type II transmembrane glycoprotein widely expressed in mammalian cells, is both a receptor/co-receptor initiating signal-transducing processes and also a multifunctional enzyme (1–3). Its known enzyme activities are synthesis from NAD⁺ of nicotinamide and of the potent calcium mobilizer

cyclic ADP-ribose (cADPR)¹ (ADP-ribosyl cyclase) and degradation of cADPR to ADP-ribose (cADPR hydrolase); in addition, CD38 has been demonstrated to catalyze a number of base-exchange reactions that include conversion of NADP⁺, in specific conditions and in the presence of nicotinic acid, to an additional calcium mobilizer, *i.e.* NAADP⁺ (4, 5).

Since the discovery of its role in cADPR metabolism, it soon became clear that CD38 is an ectoenzyme (6–11). This property raised a number of obvious questions on: (i) how the cyclase substrate NAD⁺ can become accessible to the catalytic site of CD38 at the outer surface of many cells, and (ii) even assuming ectocellular cADPR generation, how the CD38 product cADPR can reach the intracellular ryanodine-sensitive channels from which it releases calcium into the cytosol (12–15). The latter question was also supported by failure to identify any functional effect of cADPR other than its intracellular calcium releasing activity.

Similar topological questions arose for that fraction of CD38 which is localized to intracellular membrane vesicles. These mediate the export of “*de novo*” synthesized CD38 to the plasma membrane (16) and also the opposite process of CD38 endocytosis that is observed upon incubating several cell types with specific ligands, *e.g.* GSH and *N*-acetylcysteine (17, 18). In both cases, the active site of CD38 is intravesicular and therefore unavailable to cytosolic NAD⁺. Moreover, any intravesicularly generated cADPR would be sequestered inside the vesicles and therefore be unable to target the ryanodine-sensitive calcium stores.

This “topological paradox” of the CD38/cADPR system appeared to be challenging, in view of the powerful calcium releasing activity of cADPR and of the remarkably increased cytosolic calcium ([Ca²⁺]_i) levels (and consequent triggering of calcium-stimulated cell functions) that are observed during both *de novo* expression of CD38 (16) and its ligand-induced internalization (18). Both findings clearly indicated, in the absence of obvious underlying mechanisms, that intracellularly localized CD38 (*e.g.* vesicle-bound) can in fact convert cytosolic NAD⁺ to cADPR and that the cyclic nucleotide is functionally active as it can have accessibility to the calcium stores from which it up-regulates calcium release (19).

Recently, three different transporters for NAD⁺ and cADPR have been identified, which have elucidated the topological

* This work was supported by grants from the Associazione Italiana per la Ricerca sul Cancro (AIRC), Ministry for Education, University and Research-Research Projects of Relevant Interest 2000 and Ministry for Education, University and Research-National Research Council (CNR) 5% Project on Biotechnology (to A. D. F.), the University of Genova (to E. Z.), and the C.N.R. Target Project on Biotechnology (to E. Z. and C. U.). The costs of publication of this article were defrayed in part by the payment of page charges. This article must therefore be hereby marked “advertisement” in accordance with 18 U.S.C. Section 1734 solely to indicate this fact.

§ Contributed equally to the results of this work.

§§ To whom correspondence should be addressed: Department of Experimental Medicine, Section of Biochemistry, University of Genova, Viale Benedetto XV 1, 16132 Genova, Italy. Tel.: 39-010-3538155; Fax: 39-010-5221944; E-mail: toninodf@unige.it.

¹ The abbreviations used are: cADPR, cyclic ADP-ribose; NAADP⁺, nicotinic acid adenine dinucleotide phosphate; Cx43, connexin 43; DME, Dulbecco's modified Eagle's medium; PKC, protein kinase C; PKA, protein kinase A; cGDP, cyclic GDP-ribose; [Ca²⁺]_i, intracellular [Ca²⁺].

paradox of ectocellular CD38 and provided a complex model system, whereby intracellular calcium homeostasis can be regulated: (i) connexin 43 (Cx43) hemichannels proved to mediate the passive, regulated release of NAD^+ from many cells, thus potentially providing the substrate to CD38^+ cells for subsequent, ectocellular cADPR generation (20); (ii) transmembrane CD38 itself is an active transporter of catalytically generated cADPR, thus allowing cADPR to cross the cell membrane and to reach the intracellular calcium stores (21); (iii) cADPR can permeate directly across the plasma membrane of some cells, through a still molecularly undefined, yet CD38-unrelated, transport system (22). A direct interplay between Cx43 and CD38 is thus sufficient to promote an enhanced trafficking of NAD^+ (release)/cADPR (influx) across the plasma membrane.

That this functional cross-talk between CD38 and Cx43 exists also in the intracellular environment was suggested, but not yet demonstrated, by the sustained increases of $[\text{Ca}^{2+}]_i$ that are elicited by ligand-dependent endocytosis of CD38 (18, 19). Thus, CD38 and Cx43 could functionally interact in the exocytotic/endocytotic membrane vesicles which generate and release cADPR into the cytosol with subsequent calcium mobilization.

Based on these data, we addressed the occurrence of a functional interplay between Cx43 and CD38, by investigating their specific roles in the regulation of intracellular calcium. The results of this study indicated that both Cx43 and CD38 play a pivotal role in the vesicle-mediated intracellular trafficking of NAD^+ which allows substrate availability to CD38 and accordingly cADPR generation. Moreover, it became clear that availability of NAD^+ to CD38 which, if unrestricted, could damage the cell via perturbation of calcium homeostasis and NAD^+ depletion, is feedback regulated by $[\text{Ca}^{2+}]_i$. The increase of the $[\text{Ca}^{2+}]_i$ as induced by intracellular cADPR production, activates protein kinase C (PKC) which phosphorylates Cx43, resulting in its strongly decreased permeability to cytosolic NAD^+ and therefore in functional disruption of the $[\text{Ca}^{2+}]_i$ -regulating Cx43-CD38 cross-talk.

EXPERIMENTAL PROCEDURES

Materials—Cx43 antisense (5'-CTCCAGTCACCCATGTCTG-3') oligodeoxynucleotide, complementary to the AUG translation start codon region of murine Cx43 mRNA, and the corresponding sense (5'-CAGACATGGGTGACTGGAG-3') oligodeoxynucleotide were purchased from Life Technology Italia (Milan, Italy). $[\text{H}^3]$ cADPR was prepared enzymatically from $[\text{H}^3]\text{NAD}^+$ (40 Ci/mmol, PerkinElmer Life Science, Milan, Italy) with recombinant ADP-ribosyl cyclase from *Aplysia californica* (courtesy of Prof. H. C. Lee) and HPLC purified (23). Fura 2-AM, EGTA-AM, protein phosphatase inhibitors, and protein kinase inhibitors were purchased from Calbiochem (Milan, Italy). Two different antibodies were used for cytofluorimetric analyses of Cx43 (Zymed Laboratories Inc. Laboratories, San Francisco, CA): a polyclonal rabbit antibody reactive with both phosphorylated and nonphosphorylated forms of Cx-43 (catalog number 71-700, Ref. 24) and a murine monoclonal antibody, raised to a synthetic peptide corresponding to a cytoplasmic sequence of the C terminus of rat Cx43, specific for the non-phosphorylated form of Cx43 (catalog number 13-8300, Ref. 24). All other chemicals were obtained from Sigma (Milan, Italy).

Cell Cultures—NIH 3T3 cells were obtained from ATCC (Rockville, MD) and cultured as described (16). Transfection with sense (CD38^+) or antisense (CD38^-) CD38 cDNA was performed as described (16). Transfected cells were routinely maintained under geneticin (1 mg/ml) selection. All experiments were performed on CD38-sense transfected fibroblasts, expressing a cyclase activity of 8.5 ± 0.7 nmol of cGDP min/mg of protein, and on CD38-antisense transfected cells, whose cyclase activity was undetectable (16).

Fluorimetric Determination of $[\text{Ca}^{2+}]_i$ —CD38 $^-$ 3T3 cells adherent on 20-mm diameter coverslips were incubated for 4 h at 37 °C in the presence or absence of 100 μM cADPR, while both CD38 $^+$ and CD38 $^-$ (as control) cells were incubated for the same time in the presence or absence of 10 μM 8-NH $_2$ -cADPR (or 8-Br-cADPR). Cx43 sense and antisense oligodeoxynucleotides were administered at 20 μM (final concentration) to 3T3 cells adherent on the coverslips in phosphatidylcho-

line liposomes, prepared by mixing oligodeoxynucleotides with a phosphatidylcholine film in serum-free DME (20). After 16 h of culture at 37 °C, cells were re-fed with complete DME. To analyze cytosolic Ca^{2+} , cells were treated as described above, and incubated in the presence of Fura 2-AM (10 μM) for 45 min at 37 °C. Basal cytosolic calcium concentration ($[\text{Ca}^{2+}]_i$) was measured as described (16).

SDS-PAGE and Western Blot Analyses—CD38 $^+$ and CD38 $^-$ 3T3 cells were lysed in water and diluted in sample buffer (25). SDS-PAGE was performed on 10% polyacrylamide gels (25) and proteins were blotted on polyvinylidene difluoride membranes (26). Saturation of membranes and incubation with the first (either anti-Cx43 rabbit polyclonal antibody or anti-Cx43 murine monoclonal antibody) and second antibody (anti-rabbit or anti-mouse IgG, Santa Cruz Biotechnology, Santa Cruz, CA) were performed following instructions of the Amersham ECL immunodetection kit (Amersham Bioscience Inc., Italia, Milan, Italy).

Cytofluorimetric Analyses—3T3 fibroblasts from adherent cultures were recovered by mechanical scraping, washed once in DME (without phenol red), fixed in 2% paraformaldehyde for 10 min in ice and permeabilized with 0.1% saponin. Cells were then washed in phosphate-buffered saline containing 0.1% saponin and exposed to either anti-Cx43 polyclonal (5 $\mu\text{g}/\text{ml}$) or monoclonal (5 $\mu\text{g}/\text{ml}$) antibody (see "Experimental Procedures") for 30 min at 0 °C in the presence of human AB serum (1:200) to avoid nonspecific binding of the antibodies. Cells were then washed and exposed to 10 $\mu\text{g}/\text{ml}$ fluorescein isothiocyanate-conjugated anti-rabbit or anti-mouse IgG in the presence of serum. Fluorescence intensity was determined on washed samples by flow cytometry using a FACScan (Coulter, Epics XL, Milan, Italy); five thousand events were analyzed per sample. Control samples were fixed and permeabilized as described above and exposed only to the secondary antibody.

Determination of Intracellular cADPR in CD38 $^{+/-}$ 3T3 and in CD38 $^+$ 3T3 Fibroblasts Incubated with Sense and Antisense Cx43 Oligodeoxynucleotides—CD38 $^+$ -transfected 3T3 cells (10^7) were incubated in the presence of 20 μM Cx43 sense or antisense oligodeoxynucleotides in phosphatidylcholine liposomes as described above. After 16 h of incubation, cells were re-fed with complete medium for a further 24 h. CD38 $^+$ cells, either treated or untreated with oligodeoxynucleotides, and untreated CD38 $^-$ cells (as control), were washed with 10 ml of DME (without phenol red), recovered by mechanical scraping, and centrifuged at $5,000 \times g$ for 30 s. Pellets were resuspended in 300 μl of cold water and frozen at -20 °C, then thawed and sonicated in ice 1 min at 3 W (Misonix, Farmingdale, NY). A 20- μl aliquot was withdrawn for assay of protein (27), while the rest of the sample was deproteinized with 10% trichloroacetic acid (23). The cADPR content of the cell extracts was analyzed by two subsequent HPLC chromatographies after addition of trace amounts of radiolabeled $[\text{H}^3]$ cADPR (5×10^3 cpm) as internal standard (23). Identification of the cADPR peak in the cell extracts was confirmed by: (i) co-elution with the radioactive standard; (ii) comparison of the absorbance spectrum and elution time with standard cADPR, and (iii) disappearance of the corresponding peak in the matched CD38-hydrolyzed samples (23). Concentrations of intracellular cADPR were calculated from the area of the HPLC peak, taking into account the percentage of nucleotide recovery obtained with the radioactive standard.

Semi-quantitative Reverse Transcriptase-PCR—Total RNA from CD38 $^+$ and CD38 $^-$ 3T3 cells was isolated using Trizol reagent (28). RNA (5 μg) was reverse-transcribed with Moloney murine leukemia virus reverse transcriptase (Promega Italia, Milan, Italy) and oligo(dT) primers. Different amounts of reverse transcriptase reaction mixtures were subjected to PCR. The reaction mixtures contained undiluted Thermo buffer (Promega), 2.5 mM MgCl_2 , 0.2 mM dNTP, 1 unit of *Taq* DNA Polymerase (Promega), and 10 μM oligonucleotide primers specific for the different cDNAs. The primers used were: 5'-GGTAAGGATCG-CTTCTTCCCTT and 5'-TCCTGTACTTGGCTCACGTGTT for Cx43 cDNA and 5'-CAATGGTGATGACCTGGCCG AND 5'-AATGAGCTGC-GTGTGGCTCC for β -actin cDNA. The cycle numbers were 20 for β -actin, 40 for Cx43 and the annealing temperature was 58 °C. The results of PCR amplification, analyzed by agarose gel electrophoresis and ethidium bromide staining, were quantitated using Chemi Doc System (Bio-Rad, Milan, Italy).

Influx and Efflux of NAD^+ in Intact NIH 3T3 Murine Fibroblasts—Adherent CD38 $^-$ 3T3 fibroblasts (10^6) were incubated for 4 h at 37 °C in the absence (control) or presence of 100 μM cADPR, with or without each of the following protein kinase inhibitors: 1 μM staurosporin (a nonspecific inhibitor of protein kinases (29)); 0.5 μM K252c (inhibitor of both protein kinase A (PKA) and protein kinase C (PKC) (30)); 100 nM bisindolylmaleimide I (BIM I, a specific PKC inhibitor (31)); or 100 nM bisindolylmaleimide V (BIM V, an inactive analog of bisindolylmaleimide

ide I (32)); or 100 μM cell permeant, myristoylated PKC inhibitor peptide 19–27 (33). Adherent CD38⁺ 3T3 fibroblasts (10^6) were incubated for the same time in the absence (control) or presence of 10 μM 8-NH₂-cADPR (or 10 μM 8-Br-cADPR), with or without 100 nM okadaic acid (inhibitor of phosphoprotein phosphatases PP1 and PP2A, Ref. 34).

Cells, treated as described above, were then recovered by mechanical scraping and washed with DME (without phenol red). Influx was measured by suspending the cells in 200 μl of DME with or without 10 mM NAD⁺ for 5 min at 25 °C. Cells were extensively washed at the same temperature with DME (without phenol red) to reduce extracellularly added NAD⁺ to undetectable concentrations (18). Cells were then extracted in 0.3 ml of carbonate buffer (100 mM Na₂CO₃, 20 mM NaHCO₃, 10 mM nicotinamide, pH 10) and the intracellular NAD⁺ content was determined in alkaline cell extracts with an enzymatic cycling assay (18). Protein concentration was measured on 50- μl aliquots of alkaline cell extracts (27). Influx was experimentally determined by measuring the difference of intracellular NAD⁺ between cells incubated with and without NAD⁺, the former cell populations being subjected to extensive washings. NAD⁺ efflux from isolated 3T3 cells was estimated after submitting native cells to zero (control) or 10 sequential washings at 25 °C with 1.5 ml of DME (without phenol red). Efflux was quantitated as the difference between NAD⁺ present in control, unwashed cells, and in washed cells, respectively (18).

In some experiments, *e.g.* those designed to investigate the effects of protein kinase and phosphatase inhibitors, only the extent of NAD⁺ influx into cells was analyzed. However, in most experiments NAD⁺ transport was measured in either direction as described above and then referred to the starting concentration of intracellular NAD⁺ ([NAD⁺]_i). Thus, the percentages of NAD⁺ transport were calculated as shown.

$$\% \text{ of transport (influx/efflux)} = \frac{\text{transported NAD}^+}{[\text{NAD}^+]_i \text{ at zero time}} \times 100 \quad (\text{Eq. 1})$$

Chelation of Intracellular Calcium—Experiments designed to clamp intracellular calcium were performed by incubating adherent CD38[−] 3T3 fibroblasts in the presence of 10 μM EGTA-AM for 18 h at 37 °C and then by challenging these cells with 100 μM cADPR for 4 h. Cells were then subjected to the following analyses: (i) fluorimetric determination of [Ca²⁺]_i (see above); (ii) flow cytometry, using the monoclonal antibody specific for nonphosphorylated Cx43 (see “Experimental Procedures”); (iii) NAD⁺ transport assay, measured as influx of extracellular dinucleotide (see above).

RESULTS

Role of Cx43 in CD38-related Regulation of Cytosolic Calcium—Murine 3T3 fibroblasts exhibit distinctive [Ca²⁺]_i levels in their native, constitutively CD38[−] state and following transfection with human CD38 cDNA, respectively (16). The higher [Ca²⁺]_i recorded in the CD38⁺ cells (40 nM) as compared with the wild-type CD38[−] controls (20 nM) was demonstrated to be causally correlated with the presence of intracellular cADPR (16).

In an attempt to investigate whether Cx43, whose hexameric hemichannels have been shown to feature NAD⁺ transporting activity in the plasma membrane (20), is also involved in regulating [Ca²⁺]_i levels, we used CD38⁺ fibroblasts pretreated with an antisense oligodeoxynucleotide against Cx43. This reagent has been successfully used to abolish NAD⁺/cADPR-based paracrine interactions between CD38⁺ and CD38[−] 3T3 fibroblasts (22). The Cx43 antisense-treated CD38⁺ cells had a [Ca²⁺]_i of 20.5 ± 1.8 nM, *i.e.* approximately half of the levels observed in Cx43 sense oligodeoxynucleotide-treated CD38⁺ cells and comparable to the basal [Ca²⁺]_i measured in the corresponding CD38[−] cells (Fig. 1). The sharp decrease of [Ca²⁺]_i recorded in the Cx43 antisense-treated fibroblasts was paralleled by a decrease of intracellular cADPR to undetectable levels, while the concentration of this cyclic nucleotide in the corresponding Cx43 sense-treated cells was 4.8 ± 0.9 pmol/mg protein.

These findings indicate that down-regulation of Cx43 expression in the CD38⁺ cells decreases the [Ca²⁺]_i to the same values observed in Cx43-positive, but CD38[−] fibroblasts.

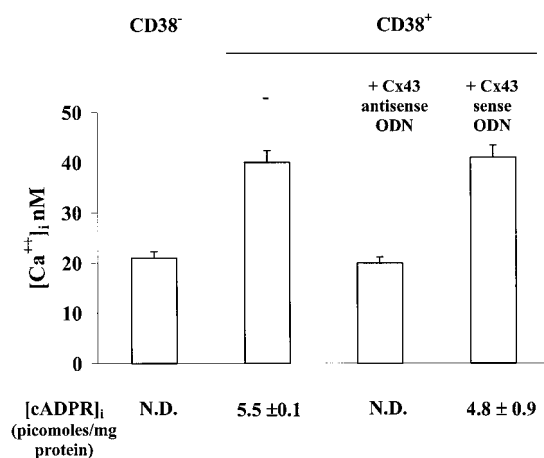


FIG. 1. Modulation of cytosolic calcium and cADPR concentrations by Cx43 antisense oligodeoxynucleotide in CD38⁺-transfected fibroblasts. CD38⁺-transfected fibroblasts were incubated in the absence or presence of either 20 μM Cx43 antisense or sense oligodeoxynucleotide as described under “Experimental Procedures.” CD38[−] fibroblasts (16) were used as control. [Ca²⁺]_i was determined fluorimetrically and [cADPR]_i was measured by HPLC analyses, as described under “Experimental Procedures.” Values are mean \pm S.D. of five different experiments. *N.D.*, not detectable.

Therefore, lack of expression of either CD38 or Cx43 leads to a remarkably lower [Ca²⁺]_i than measured in cells expressing both proteins, due to disappearance of intracellular cADPR.

Cx43-mediated NAD⁺ Transport in CD38[−] and CD38⁺ 3T3 Fibroblasts—The plasma membrane of native 3T3 fibroblasts, as well as that of other cell types, harbors Cx43 hemichannels that can mediate a pH-dependent, temperature-independent, bidirectional NAD⁺ transport down a concentration gradient (20). In view of the high intracellular and quite low extracellular NAD⁺ concentrations (18), release of NAD⁺ from cells should be largely favored over influx.

Earlier experiments had indicated that Cx43-mediated NAD⁺ transport is inhibited in a concentration-dependent fashion by extracellular as well as by intracellular calcium (20). Therefore, we investigated the correlation between CD38-dependent, cADPR-mediated, changes of [Ca²⁺]_i levels in 3T3 fibroblasts and the corresponding NAD⁺ transporting activities across the plasma membrane, measured both as influx and efflux of the dinucleotide. Results shown in Table I indicate that maximum NAD⁺ transport occurs in native CD38[−] 3T3 fibroblasts where the [Ca²⁺]_i is ~ 20 nM. Specifically, release of 35% of total NAD⁺ from cells reflects the total fraction of exchangeable pyridine dinucleotide, most likely identifiable with cytosolic, nonprotein-bound NAD⁺ (18). On its turn, an influx accounting for 70% was measured in the CD38[−] cells: this value might be slightly underestimated because of the requirement to wash cells following incubation with added NAD⁺ to remove the extracellular and surface-bound dinucleotide (18) and of consequent partial loss of intracellular NAD⁺. By comparison, the CD38⁺ 3T3 cells, whose [Ca²⁺]_i was ~ 40 nM, consistently exhibited a remarkably decreased NAD⁺ transport, notably dinucleotide efflux (1.3%), but also its influx (29%).

The inverse correlation between CD38 expression and NAD⁺ transport (Table I) could be due to either of two possibilities: (i) a distinctive abundance of Cx43 in the CD38[−] (unrestrained dinucleotide transport) *versus* the CD38⁺ fibroblasts (featuring a comparatively lower NAD⁺ transport); (ii) a different post-biosynthetic regulation of Cx43-mediated NAD⁺ transport in the CD38[−] *versus* the CD38⁺ fibroblasts. Therefore, we first compared the expression of Cx43 in the CD38[−] and CD38⁺ cells, using a polyclonal antibody that cross-reacts with both

TABLE I
NAD⁺ transport through plasmamembrane Cx43 hemichannels in
CD38⁺ and CD38⁻ 3T3 murine fibroblasts

Cell type	[Ca ²⁺] _i	NAD ⁺ efflux ^a	NAD ⁺ influx ^a
	<i>nM</i>		<i>%</i>
CD38 ⁻ 3T3	20.5 ± 1.8	34.5 ± 4.7	69.8 ± 5.8
CD38 ⁺ 3T3	40.2 ± 3.2	1.3 ± 0.5	28.9 ± 3.3

^a Measured as percentages of transported NAD⁺ relative to total [NAD⁺]_i at zero time (see "Experimental Procedures").

phosphorylated and nonphosphorylated Cx43 (see "Experimental Procedures"). As shown in Fig. 2A, Western blot experiments did not demonstrate any appreciable quantitative difference of Cx43 content between lysates from CD38⁻ and CD38⁺ cells. Moreover, cytofluorimetric analyses of saponin-permeabilized cells showed a superimposable pattern of total Cx43 expression in the CD38⁻ and CD38⁺ cell populations (Fig. 2B). Finally, semiquantitative PCR analysis of the two types of fibroblasts indicated a closely comparable abundance of Cx43 mRNA (Fig. 2C). Altogether, these evidences indicate that CD38⁻ and CD38⁺ cells express comparable amounts of Cx43 (see "Discussion").

Cx43 is known to occur in phosphorylated as well as in nonphosphorylated forms (reviewed in Refs. 35 and 36). Several lines of evidence suggest that the state of phosphorylation can modulate Cx43 trafficking, assembly/disassembly in gap junctional plaques, turnover, degradation, and gating (36). Cx43 features multiple phosphorylation sites targeted by different protein kinases and affording a pleiotropic control on gap junction communication. Therefore, CD38⁻ and CD38⁺ 3T3 fibroblasts, exhibiting unrestrained and inhibited NAD⁺ transport across their plasma membranes, respectively (Table I), were analyzed for their content of nonphosphorylated/phosphorylated Cx43, using a monoclonal antibody specific for the nonphosphorylated form. This antibody was raised against a peptide comprising amino acid residues 360–376 of the Cx43 sequence (24), which contains the protein kinase C (PKC) sites of phosphorylation, *i.e.* Ser-368 and Ser-372 (36).

As shown in Fig. 3, use of this specific monoclonal antibody revealed a significant difference ($p < 0.01$) between CD38⁻ and CD38⁺ cells. Thus, with measurably comparable amounts of total Cx43 protein in the two cell types (Fig. 2), the CD38⁻ cells exhibited more nonphosphorylated Cx43 than the corresponding CD38⁺ cells. This difference, although limited in extent (see "Discussion"), is in fact related to control [Ca²⁺]_i levels (Table I). Moreover, since it functionally corresponds to the measured transition from an open to a virtually closed state of plasma membrane Cx43 hemichannels (Table I), it seems to represent a mechanism designed to avoid depletion of intracellular NAD⁺.

Calcium-mediated Effects of Extracellular cADPR on the NAD⁺ Transport of CD38⁻ 3T3 Fibroblasts—*De novo* expression of CD38 in constitutively CD38⁻ 3T3 fibroblasts results in remarkable changes in the biochemical properties of these cells which are ultimately triggered by appearance of intracellular cADPR (16). Therefore, we investigated whether the differences in the structural and functional properties of Cx43 in the CD38⁻ and CD38⁺ 3T3 fibroblasts, respectively, can be reproduced upon directly loading the CD38⁻ cells with cADPR. This approach was made feasible by the recent finding that 3T3 fibroblasts express on their plasma membrane a cADPR-transporting system, whose molecular characterization is underway,² which determines influx of extracellular cADPR into these cells (22).

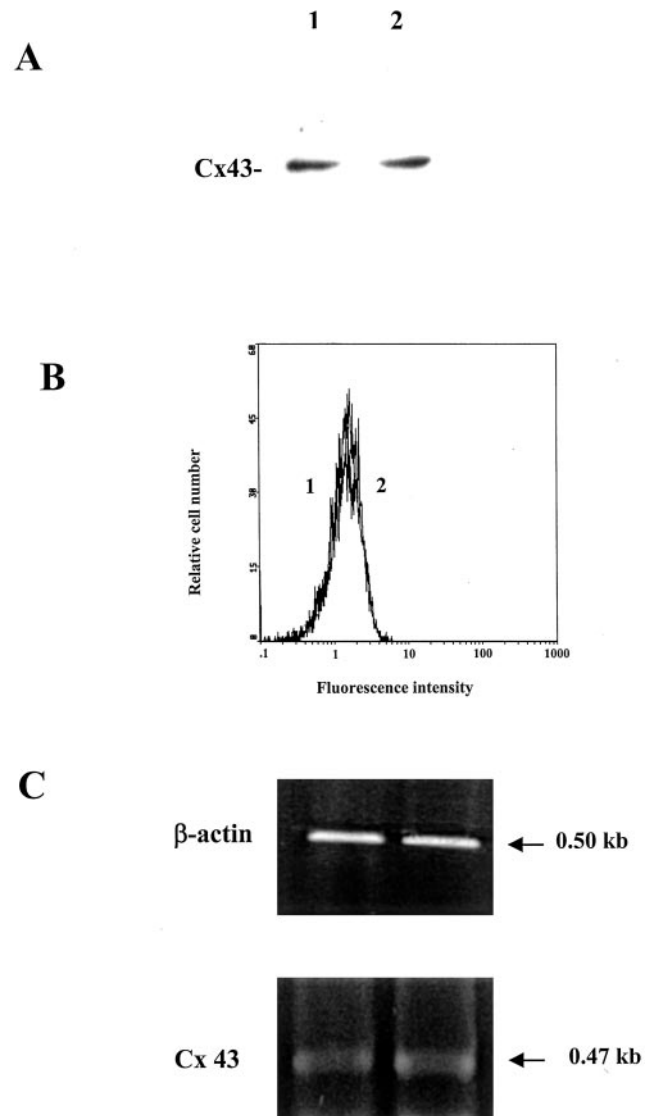


FIG. 2. Cx43 expression in CD38⁺ and CD38⁻ 3T3 fibroblasts. A, Western blot analysis (one of four) of CD38⁺ (lane 1) and CD38⁻ (lane 2) 3T3 fibroblasts. SDS-PAGE and immunodetection of Cx43 (both phosphorylated and nonphosphorylated forms) were performed as described under "Experimental Procedures," using a polyclonal rabbit anti-Cx43 antibody (24). B, cytofluorimetric analysis (one representative experiment of five) of CD38⁺ (1) and CD38⁻ (2) 3T3 fibroblasts. Cells were fixed, permeabilized, exposed to a polyclonal rabbit anti-Cx43 antibody and a secondary fluorescein isothiocyanate-conjugated anti-rabbit antibody as described under "Experimental Procedures." C, semiquantitative reverse-transcribed PCR amplification, analyzed by agarose gel electrophoresis and ethidium bromide staining. RNA from CD38⁺ (1) and CD38⁻ (2) 3T3 fibroblasts was reverse transcribed and cDNA was subjected to PCR reaction using Cx43 and β -actin-specific primers.

We first compared the NAD⁺ transporting activity, measured both as influx and as release of the dinucleotide, in the cADPR-loaded and unloaded CD38⁻ cells, respectively (Fig. 4). Exposure of cells to 100 μ M extracellular cADPR for 4 h resulted in an increase of [Ca²⁺]_i levels from 20 ± 1 to 50 ± 3 nM (Fig. 4A), confirming previous results (22). Concomitantly to increased [Ca²⁺]_i levels, the cADPR-loaded fibroblasts showed a remarkably decreased NAD⁺ efflux (approximately half of that recorded in the unloaded cells) and influx of extracellular NAD⁺ (approximately one-third). Therefore, the extent of NAD⁺ influx into the cADPR-loaded cells was low, being almost equivalent to that observed in the CD38-transfected cells (Table I). NAD⁺ efflux was not as low as in the CD38⁺ cells,

² L. Guida, L. Sturla, and A. De Flora, unpublished observations.

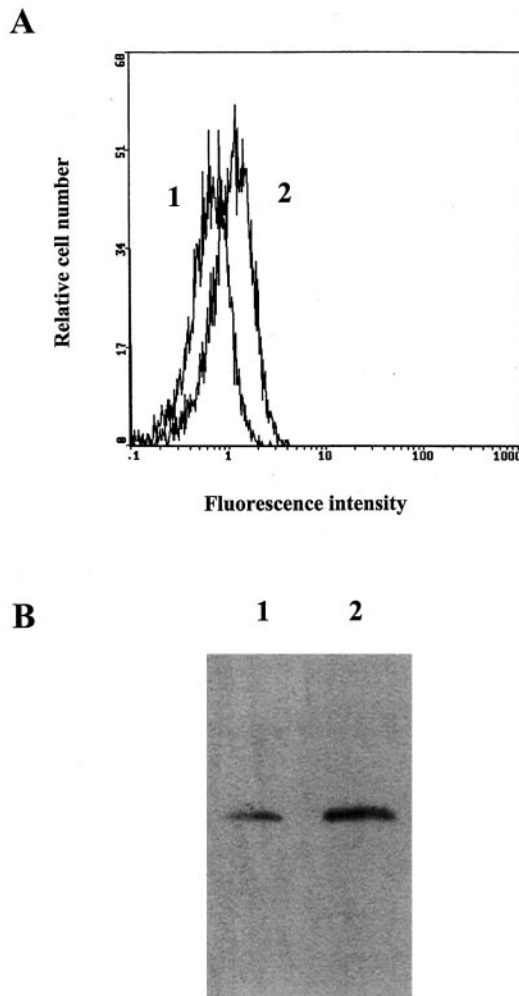


FIG. 3. Comparative expression of nonphosphorylated Cx43 in CD38⁻ and CD38⁺ 3T3 fibroblasts. A, CD38⁺ (1) and CD38⁻ (2) fibroblasts were fixed, permeabilized, exposed to a monoclonal anti-Cx43 antibody specific for the nonphosphorylated form (24) and then to fluorescein isothiocyanate-conjugated secondary anti-mouse antibody as described under "Experimental Procedures." The fluorescence intensity of the samples was analyzed by flow cytometry; results of a representative experiment (one of six, yielding closely comparable results) are shown. B, Western blot analysis (one of five) of CD38⁺ (1) and CD38⁻ (2) 3T3 fibroblasts. SDS-PAGE and immunoblotting of Cx43 nonphosphorylated form were performed using a monoclonal anti-Cx43 antibody (24), as described under "Experimental Procedures."

although being significantly restrained as compared with the native CD38⁻ fibroblasts. This quantitative difference of NAD⁺ release consistently measured in the cADPR-loaded CD38⁻ cells and in CD38⁺ cells, respectively, could be due to a reduced gradient between intracellular and extracellular NAD⁺ in the CD38-transfected fibroblasts. Indeed, these cells have a significantly lower NAD⁺ content, due to its CD38-catalyzed consumption, than native, untransfected (or CD38 antisense-transduced) 3T3 cells (16), which may account for a comparatively decreased NAD⁺ efflux. In any case, the presence of intracellular cADPR, either as a result of CD38 transfection or of direct loading into CD38⁻ cells, shows a sharp correlation with high [Ca²⁺]_i levels and low NAD⁺-transporting efficiency across the plasma membrane.

To investigate the structural basis of the differences between native and cADPR-loaded CD38⁻ cells in terms of transmembrane NAD⁺ fluxes, we comparatively analyzed the ratio between nonphosphorylated and PKC-phosphorylated Cx43 forms in the two cell populations. Inspection of Fig. 5 shows a lower content of nonphosphorylated Cx43 in the cADPR-loaded

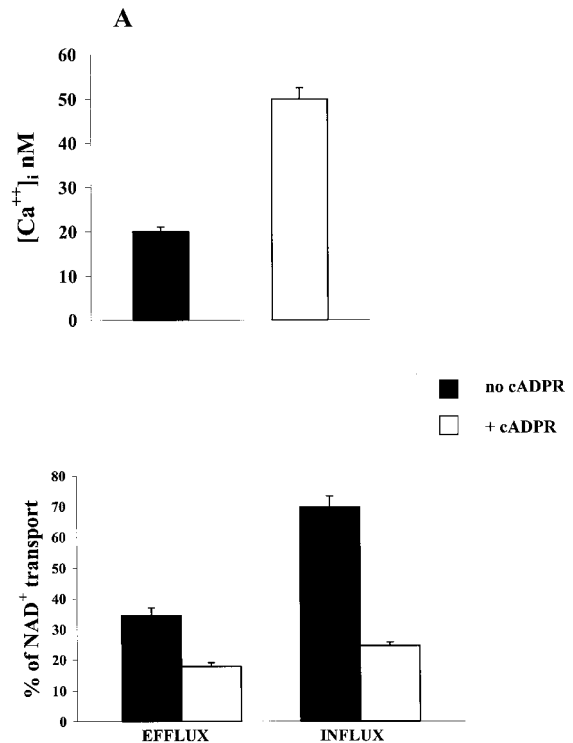


FIG. 4. Effects of extracellularly added cADPR on cytosolic calcium levels and on NAD⁺ transport in CD38⁻ fibroblasts. CD38⁻ 3T3 cells were incubated in the absence (black columns) or presence of 100 μ M cADPR (white columns) for 4 h at 37 $^{\circ}$ C. A, [Ca²⁺]_i was determined fluorimetrically; values are mean \pm S.D. of five different experiments. B, NAD⁺ transporting activities (measured both as influx and as efflux as described under "Experimental Procedures") are indicated on the ordinate as percentages of transported NAD⁺ relative to the total intracellular NAD⁺ at zero time. Values are mean \pm S.D. of 10 different experiments.

(trace 1) than in the native 3T3 fibroblasts (trace 2) ($p < 0.01$). Conversely, the two cell populations consistently exhibited an identical content of total Cx43 (*i.e.* the sum of phosphorylated and nonphosphorylated Cx43) (not shown). Accordingly, this specific difference of nonphosphorylated Cx43 is in the same direction as that between CD38⁻ and CD38⁺ cells, with the native control cells exhibiting low [Ca²⁺]_i, high NAD⁺ transport, and more nonphosphorylated Cx43 than the CD38⁺ cells featuring high [Ca²⁺]_i and decreased NAD⁺ fluxes (see "Discussion").

In an effort to causally correlate changes in Cx43 phosphorylation and transmembrane NAD⁺ transport to cADPR-induced variations of the [Ca²⁺]_i levels, we performed experiments aiming to minimize these variations by means of the permeant calcium chelator EGTA-AM. Following preincubation of CD38⁻ fibroblasts with 10 μ M EGTA-AM for 18 h (see "Experimental Procedures"), the [Ca²⁺]_i levels dropped to 11 ± 2 nM. Subsequent addition of 100 μ M cADPR to the EGTA-AM-treated cells did not elicit any [Ca²⁺]_i increase above these low levels, which proved to be poorly compatible with cell survival. In any case, NAD⁺ transport, measured as influx of dinucleotide into the EGTA-AM-treated fibroblasts, was 93% of that recorded in the untreated cells (without EGTA-AM). Moreover, subsequent exposure to extracellular cADPR after EGTA-AM treatment did not induce any modification either in the transporting activity (90% influx compared with untreated cells), or in the extent of Cx43 phosphorylation as detected by flow cytometry analyses. These results clearly implicate the cADPR-induced changes of [Ca²⁺]_i as responsible for the observed changes in NAD⁺ transport and in the underlying process of Cx43 phosphorylation.

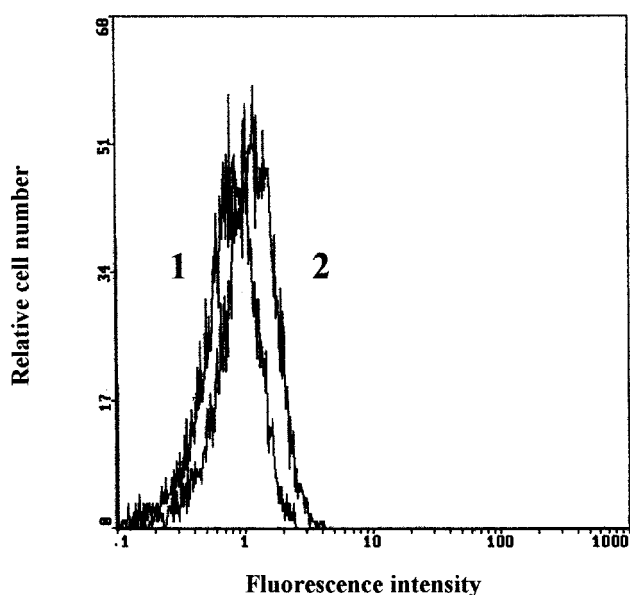


FIG. 5. Comparative expression of nonphosphorylated Cx43 in native and cADPR-loaded CD38⁻ 3T3 fibroblasts. Adherent CD38⁻ 3T3 fibroblasts were incubated in the presence (1) or absence (2) of 100 μ M cADPR for 4 h at 37 °C. Cells were collected, fixed, and permeabilized as described under "Experimental Procedures." Exposure to the monoclonal anti-Cx43 antibody (24), to subsequent fluorescein isothiocyanate-conjugated anti-mouse antibody and flow cytometry analyses were performed as described under "Experimental Procedures." Results of a representative experiment (one of six, yielding closely comparable results) are shown.

Effect of 8-NH₂-cADPR on the NAD⁺ Transport—To unequivocally demonstrate the inverse correlation between cADPR-dependent $[Ca^{2+}]_i$ increases and inhibition of NAD⁺ transport across Cx43 hemichannels, we explored this transporting activity in the plasma membrane of CD38⁺ fibroblasts preliminarily exposed to 8-NH₂-cADPR. This cADPR analog (37) can antagonize the calcium mobilizing activity of cADPR when supplemented in the extracellular medium (22). Indeed, the 8-NH₂-cADPR-challenged cells had comparatively lower $[Ca^{2+}]_i$ levels than the untreated CD38⁺ fibroblasts (Fig. 6A). Their NAD⁺ transporting activity was much higher than that measured in the untreated CD38⁺ cells (Fig. 6B). Specifically, the extent of influx (~64%) was comparable to the unrestrained one recorded in the native CD38⁻ cells (70%, see Table I), while the efflux (~12%) was still remarkably greater than that measured in the untreated CD38⁺ fibroblasts (1.3%, see Table I). These data indicate that 8-NH₂-cADPR, which inhibits the calcium releasing activity of cADPR, prevents the cADPR-induced decrease of NAD⁺ transport.

Role of Protein Kinase C in the NAD⁺ Transport Mediated by Cx43 Hemichannels—Phosphorylated versus nonphosphorylated Cx43 channels and hemichannels are known to feature remarkably different activities of solute exchange, which are also differentially regulated by the multiple sites of phosphorylation recognized by the several protein kinases acting on Cx43 (35, 36, 38, 39). Moreover, although this effect was observed in a quite restricted range of expression of nonphosphorylated Cx43 (see "Discussion"), also the specific NAD⁺ transporting activity is much higher in the native CD38⁻ cells than in the same cADPR-loaded cells or in the CD38⁺ fibroblasts. To address the role and the mechanisms of Cx43 phosphorylation/dephosphorylation on NAD⁺ transport in CD38⁺ and CD38⁻ cells, we started experiments with protein kinase and phosphatase inhibitors, in which transport of NAD⁺ was measured as influx of the dinucleotide into the variously treated cell samples. Fig. 7 shows that okadaic acid, an inhibitor of phospho-

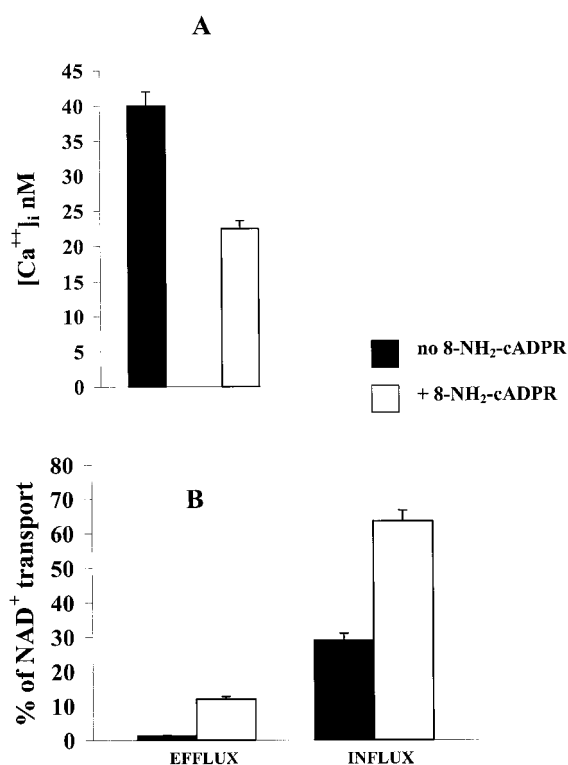


FIG. 6. Effect of the cADPR antagonist 8-NH₂-cADPR on cytosolic calcium levels and on transmembrane NAD⁺ transport in CD38⁺ fibroblasts. CD38⁺ 3T3 fibroblasts were incubated without (black columns) or with 10 μ M of the cADPR analog and antagonist 8-NH₂-cADPR (37) (white columns), for 4 h at 37 °C. A, $[Ca^{2+}]_i$ was determined fluorimetrically and values are mean \pm S.D. of five different experiments. B, NAD⁺ influx and efflux from intact cells are indicated as reported under "Experimental Procedures." Values are mean \pm S.D. of eight different experiments.

protein phosphatases PP1 and PP2A (hydrolyzing phosphate esters of serine and threonine residues), but not of phosphotyrosine phosphatases (34), completely abrogates the effect afforded by 8-NH₂-cADPR on the NAD⁺ transporting activity of the CD38⁺ cells, *i.e.* enhancement of NAD⁺ influx over untreated control cells (see also Fig. 6). Similar results were obtained in experiments where another cADPR analog and antagonist, 8-Br-cADPR (37), was used instead of 8-NH₂-cADPR. Therefore, maintenance of Cx43 in its phosphorylated form, incompetent for NAD⁺ transport, prevents the CD38⁺ cells from becoming responsive to the cADPR antagonist via a reduced $[Ca^{2+}]_i$. This finding indicates that in the CD38⁺ fibroblasts the increased permeability of Cx43 hemichannels to NAD⁺ which follows the 8-NH₂-cADPR-dependent $[Ca^{2+}]_i$ decrease occurs via Cx43 dephosphorylation.

Based on this result and on the apparent role of PKC-phosphorylated Cx43 in decreasing NAD⁺ transport (Table I and Fig. 3), we addressed in a more systematic way the role of various protein kinases on NAD⁺ influx into CD38⁻ 3T3 fibroblasts. As shown in Fig. 8, while extracellular cADPR substantially decreased the NAD⁺ transport (in agreement with experiments illustrated in Fig. 4), staurosporin, a nonspecific inhibitor of protein kinases (29), abolished this inhibiting effect of cADPR almost completely. The same result was elicited in the cADPR-loaded CD38⁻ cells by K252c (inhibiting both PKA and PKC, Ref. 30), by bisindolylmaleimide I (a specific PKC inhibitor, Ref. 31) but not by the inactive (*i.e.* non PKC-inhibiting) analog bisindolylmaleimide (32), and also by a permeant myristoylated peptide that specifically inhibits PKC (33). Altogether, these results implicate PKC as responsible for the extraphosphorylation of Cx43 hemichannels that characterizes

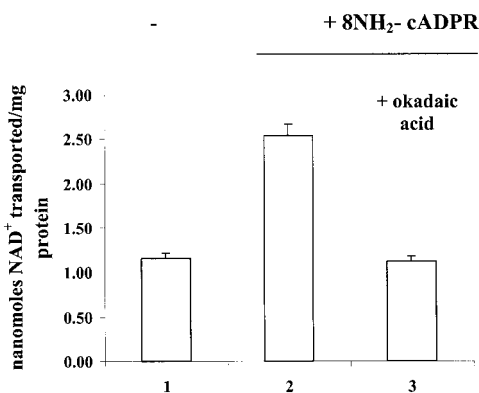


FIG. 7. Influx of NAD⁺ into CD38⁺ fibroblasts in the presence of 8-NH₂-cADPR and okadaic acid. CD38⁺ fibroblasts were incubated in the absence (1) or presence of 10 μ M 8-NH₂-cADPR, without (2) or with 100 nM okadaic acid (3), for 4 h at 37 °C. NAD⁺ influx was performed as described under "Experimental Procedures." Values are mean \pm S.D. of five different experiments. CD38⁺ cells incubated in the presence of okadaic acid alone showed the same NAD⁺ influx as CD38⁺ cells (not shown).

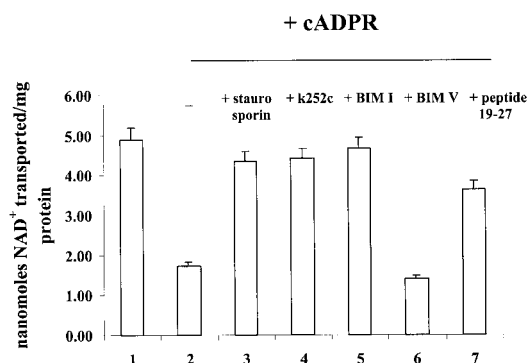


FIG. 8. Influx of NAD⁺ into CD38⁻ fibroblasts in the presence of cADPR and various protein kinase inhibitors. CD38⁻ fibroblasts were incubated in the absence (1) or presence of 100 μ M cADPR, without (2) or with 1 μ M staurosporin (3), 0.5 μ M K252c (4), 100 nM BIM I (5), 100 nM BIM V (6), or 100 μ M myristoylated PKC peptide 19–27 inhibitor (7). NAD⁺ influx was measured on each sample as described under "Experimental Procedures." Values are mean \pm S.D. of four different experiments. None of these inhibitors incubated with CD38⁻ cells without cADPR proved to interfere with NAD⁺ influx (not shown).

the CD38⁺ cells distinctively from the CD38⁻ cells and that functionally restrains NAD⁺ transport either in the CD38⁺ fibroblasts or in the cADPR-loaded CD38⁻ cells.

DISCUSSION

Cx43 hemichannels, recently demonstrated to be responsible for NAD⁺ transport across the plasma membrane (20), have been recognized to play an important role in mediating a paracrine exchange of NAD⁺ and cADPR between neighboring cells. Specifically, in several heterotypic cell systems, Cx43 hemichannels proved to release NAD⁺ from "stromal" cells, thereby enabling the generation of cADPR in the extracellular environment and the subsequent response of adjacent "parenchymal" cells to this cyclic nucleotide in terms of calcium mobilization and triggering of calcium-controlled cell-specific responses. These paracrine patterns have been identified on: (i) bovine tracheal mucosal cells/smooth myocytes, with a cADPR-dependent, calcium-mediated, acetylcholine-induced contractility being observed in intact tissue fragments (40); (ii) CD38⁺/CD38⁻ 3T3 murine fibroblasts, with an increased proliferation, due to shortening of the S phase of cycle, of the CD38⁻ cells co-cultured with CD38⁺ feeders (22); (iii) stromal cells/human hemopoietic progenitors, with mixed transwell co-cultures showing a significant, cADPR-mediated and calcium-depend-

ent expansion of the HP (41); (iv) rat astrocytes/hippocampal neurons, the former cells featuring a cADPR-induced glutamate release which triggers calcium responses in neurons (42).

The aim of the present study was to address whether a functional cross-talk between Cx43 and CD38 can also occur within the same cell, thereby triggering an autocrine process based upon intracellular trafficking of NAD⁺ and cADPR and resulting in an increase of [Ca²⁺]_i levels, as suggested by earlier findings (16, 18). The functional interplay between Cx43 and CD38 was demonstrated by the fact that both transmembrane proteins were required to determine high [Ca²⁺]_i levels via intracellular cADPR generation (Fig. 1). Our results support the view that, besides doing so at the plasma membrane level, Cx43 and CD38 play concerted and interacting roles also in the intracellular membrane vesicles. Preliminary experiments of subcellular co-localization by means of confocal microscopy, immunofluorescence, and cryoimmunoelectron microscopy were unsuccessful because of the inadequacy of the anti-Cx43 antibodies to detect the low amounts of Cx43 expressed in 3T3 fibroblasts (Figs. 2, 3, and 5). Nevertheless, the present biochemical data, together with earlier results (16, 18, 21), indicate that both transmembrane proteins mediate topologically opposite fluxes of NAD⁺ and cADPR between subcellular compartments, with Cx43 determining a passive, inward directed transport of cytosolic NAD⁺ into the vesicles and with CD38 catalyzing the intravesicular generation and the active outpumping of cADPR into the cytosol. That this intense trafficking of NAD⁺ and cADPR is related to intracellular rather than to ectocellular CD38 is demonstrated by our failure to observe significant decreases of the [Ca²⁺]_i upon supplementation of NAD⁺-glycohydrolase to the culture media of CD38⁺ 3T3 fibroblasts (not shown). On the contrary, extracellularly added NAD⁺-glycohydrolase proved to be effective in abrogating cell-to-cell interactions in mixed co-cultures of CD38⁺/CD38⁻ 3T3 fibroblasts (22), thereby implicating Cx43-mediated NAD⁺ release across the plasma membrane of the CD38⁺ cells.

On the whole, this complex process of subcellular (di)nucleotide compartmentation *per se* (Fig. 9) can be considered as a way to prevent unrestrained NAD⁺ consumption and excessive cADPR generation, which could result in the accumulation of cytosolic Ca²⁺ potentially eliciting cytotoxic effects (43). However, such topological compartmentation of NAD⁺ and cADPR might not be sufficient to prevent high [Ca²⁺]_i levels and their detrimental consequences, if the vesicle-bound Cx43 hemichannels were in an open state enabling free access of cytosolic NAD⁺ to the intravesicular active site of CD38 and hence virtually unrestricted cADPR generation.

Therefore, the inhibitory effect of Ca²⁺ on Cx43-mediated NAD⁺ transport (Table I) can be considered as a feedback mechanism designed to down-regulate the subcellular trafficking of NAD⁺ and cADPR between cytosol and membrane vesicles, and accordingly to avoid potentially dangerous accumulation of [Ca²⁺]_i. That this self-regulatory mechanism driven by calcium itself can have a physiological role is strongly suggested by the fact that even under conditions of extensive ligand-induced internalization of plasma membrane-bound CD38 (up to 80% of ectocellular cyclase activity), the accompanying sustained increase of [Ca²⁺]_i tends to plateau at ~90–100 nM [Ca²⁺]_i (18).

Self-regulation of the NAD⁺/cADPR system by means of inhibition of the Cx43/CD38 cross-talk by high [Ca²⁺]_i is not directly afforded by Ca²⁺ itself or Ca²⁺-calmodulin. This became clear when influx of NAD⁺ into proteoliposomes that had been reconstituted with Cx43 (20) proved to be completely unaffected by either calmodulin or Ca²⁺-calmodulin (not

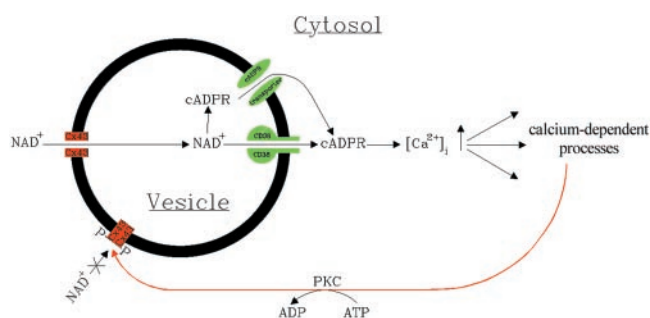


FIG. 9. Ca^{2+} -stimulated, PKC-catalyzed phosphorylation of connexin 43 down-regulates the Cx43-CD38 cross-talk and avoids excessive $[\text{Ca}^{2+}]_i$ increases. Topological and functional interactions between Cx43 hemichannels, CD38, and the cADPR transporter (22) regulate the intracellular NAD^+ and cADPR metabolism at the level of vesicles/cytosol. Permeability of cytosolic NAD^+ across non-phosphorylated Cx43 is followed by intravesicular generation of cADPR and by its efflux to the cytosol to reach the target calcium stores. The subsequent increase of $[\text{Ca}^{2+}]_i$ triggers calcium-dependent processes including PKC-mediated phosphorylation of Cx43 hemichannels in the vesicle: this results in the impermeability of Cx43 to cytosolic NAD^+ and accordingly in the blockade of further $[\text{Ca}^{2+}]_i$ increases. This self-regulatory loop providing a decreased NAD^+ and cADPR metabolism sets the threshold of $[\text{Ca}^{2+}]_i$ above which calcium-dependent cytotoxic effects would be switched on.

shown). This negative result compares well with the lack of calmodulin-binding domains in the Cx43 structure, while calmodulin-binding sequences are present, for example, in Cx32 (44, 45). On the other hand, the slight but significantly distinctive ratios of PKC-phosphorylated to nonphosphorylated Cx43 in CD38^+ and in CD38^- cells, that correspond to Ca^{2+} -related closure or opening, respectively, of the Cx43 hemichannels to NAD^+ transport (Table I and Fig. 3), prompted us to investigate the possibility of an effect of intracellular calcium on protein kinases/phosphatases. This was also suggested by the known fact that, although several protein kinases recognize Cx43 as substrate at different phosphorylation sites, PKC is the only one which has been unequivocally demonstrated to decrease gap junctional coupling of this specific connexin (36). Our experiments showed that indeed calcium-stimulated PKC is the specific trigger for lowering the activity of Cx43 as NAD^+ transporter (Fig. 8).

NAD^+ fluxes proved to be switched off and on, respectively, over a narrow range of the ratio between the phosphorylated (closed) and the nonphosphorylated (open) Cx43 forms. Quantitative values derived from the corresponding cytofluorimetric analyses with the polyclonal (Fig. 2B) and the monoclonal (Fig. 3A) anti-Cx43 antibodies indicated that the native CD38^- 3T3 fibroblasts contain approximately 5-fold more phosphorylated than nonphosphorylated Cx43. Either transfection with CD38 (Fig. 3) or cADPR loading into the cells (Fig. 5) increased the content of PKC-phosphorylated Cx43 even further, thus making Cx43 almost impermeable to NAD^+ fluxes. It is possible that the apparently limited difference of phosphorylated Cx43 species, accounting for large differences in NAD^+ transport, is in fact greater than measured by cytofluorimetric analyses on fully permeabilized cells. These experiments yielded "total" intracellular Cx43 (both as phosphorylated and nonphosphorylated forms). Therefore, the proportions of nonphosphorylated Cx43 in distinct subcellular pools playing a role in NAD^+ transport (e.g. endoplasmic reticulum, mitochondria and the plasma membrane) might be distinctly different from those estimated on total cellular Cx43.

Whichever the explanation, a clear inverse correlation exists between efficiency of NAD^+ transport and PKC-mediated Cx43 phosphorylation. Therefore, this regulatory mechanism related to Cx43 phosphorylation seems to be provided with an exquis-

ite sensitivity to $[\text{Ca}^{2+}]_i$ levels, as also shown by its disruption following chelation of intracellular calcium by cell-permeant EGTA-AM. Besides representing a means for control of intracellular calcium homeostasis via a fine modulation of intracellular NAD^+ fluxes, PKC-mediated phosphorylation of Cx43 might prevent release of cytosolic NAD^+ from cells and accordingly down-regulate the recently identified paracrine processes involving enhanced trafficking of NAD^+ and cADPR (22, 40–42).

Modulation of the subcellular trafficking of NAD^+ has a recently described precedent based upon the function of the permeability transition pore (46) in rat heart mitochondria. In this cell system, opening of the permeability transition pore (reminiscent of opening of Cx43 hemichannels) causes the release of mitochondrial NAD^+ , making it available to the otherwise inaccessible NAD^+ -glycohydrolase localized outside the matrix space (47). Interestingly, mitochondrial NAD^+ -glycohydrolase has been found to express ADP-ribosyl cyclase activity (48). Therefore, in cardiomyocytes the mitochondrial compartment can release NAD^+ , possibly to promote generation of functionally active cADPR with an increase of $[\text{Ca}^{2+}]_i$ levels. Blockade of permeability transition pore opening protected mitochondria from NAD^+ depletion. A further and striking analogy with our cell system is that efflux of NAD^+ from mitochondria can determine extensive release of the dinucleotide from cells, as observed under conditions of postischemic reperfusion of cardiomyocytes that resulted in sarcolemmal rupture (47). Thus, as reported in 3T3 fibroblasts, both a subcellular trafficking and a release of NAD^+ from rat heart myocytes have been demonstrated.

Fig. 9 summarizes the cross-talk between CD38 and Cx43 identified in the present study. This scheme represents an oversimplification, as the proportion of NAD^+ -impermeable, phosphorylated Cx43 is in fact much higher than that of open, nonphosphorylated Cx43. In conclusion, CD38 is a component of an exceedingly complex self-regulatory system which, through functional interactions with other proteins including Cx43 and the transmembrane cADPR transporter, fits all requirements expected for ensuring subtle control of intracellular calcium homeostasis in cADPR-responsive cell types (49). It should be mentioned, to this purpose, that, although this novel regulatory system is triggered by $[\text{Ca}^{2+}]_i$ variations in the physiological range (16), the eventual result is the prevention of severe imbalances of intracellular calcium homeostasis. Additional mechanisms may be involved in the system illustrated in Fig. 9, e.g. Cx43 dephosphorylation, possible effects of Cx43 phosphorylation/dephosphorylation on stability of this connexin (36, 50), other protein kinases, as yet undefined long-term effects suggested by quantitative differences between CD38 transfection and simple loading of cADPR in the CD38^- cells (Ref. 22 and this study). In any case, analysis of individual steps of this novel signaling cascade identifies several potential targets of naturally occurring modulators and of *ad hoc* designed drugs for selectively regulating intracellular calcium levels and calcium-dependent processes.

REFERENCES

- Jackson, D. G., and Bell, J. I. (1990) *J. Immunol.* **144**, 2811–2815
- Mehta, K., Shahid, U., and Malavasi, F. (1996) *FASEB J.* **10**, 1408–1417
- Mehta, K., and Malavasi, F. (2000) *Human CD38 and Related Molecules*, Karger, Basel, Switzerland
- Aarhus, R., Graeff, R. M., Dickey, D. M., Walseth, T. F., and Lee, H. C. (1995) *J. Biol. Chem.* **270**, 30327–30334
- Lee, H. C. (2001) *Annu. Rev. Pharmacol. Toxicol.* **41**, 317–345
- States, D. J., Walseth, T. F., and Lee, H. C. (1992) *Trends Biochem. Sci.* **17**, 495
- Howard, M., Grimaldi, J. C., Bazan, J. F., Lund, F. E., Santos-Argumedo, L., Parkhouse, R. M., Walseth, T. F., and Lee, H. C. (1993) *Science* **262**, 1056–1059
- Lee, H. C., Zocchi, E., Guida, L., Franco, L., Benatti, U., and De Flora, A. (1993) *Biochem. Biophys. Res. Commun.* **191**, 639–645
- Kontani, K., Nishina, H., Ohoka, Y., Takahashi, K., and Katada, T. (1993)

- J. Biol. Chem.* **268**, 16895–16898
10. Takasawa, S., Tohgo, A., Noguchi, N., Koguma, T., Nata, K., Sugimoto, T., Yonekura, H., and Okamoto, H. (1993) *J. Biol. Chem.* **268**, 26052–26054
 11. Summerhill, R. J., Jackson, D. G., and Galione, A. (1993) *FEBS Lett.* **355**, 231–233
 12. Lee, H. C., Graeff, R. M., and Walseth, T. F. (1995) *Biochimie (Paris)* **77**, 345–355
 13. Lund, F., Solvason, N., Grimaldi, J. C., Parkhouse, M. E., and Howard, M. (1995) *Immunol. Today* **16**, 469–473
 14. De Flora, A., Guida, L., Franco, L., and Zocchi, E. (1997) *Int. J. Biochem. Cell Biol.* **29**, 1149–1166
 15. Adebajo, O. A., Shankar, V. S., Pazianas, M., Simon, B. J., Lai, F. A., Huang, C. L. H., and Zaidi, M. (1996) *Am. J. Physiol.* **271**, F469–F475
 16. Zocchi, E., Daga, A., Usai, C., Franco, L., Guida, L., Bruzzone, S., Costa, A., Marchetti, C., and De Flora, A. (1998) *J. Biol. Chem.* **273**, 8017–8024
 17. Zocchi, E., Franco, L., Guida, L., Piccini, D., Tacchetti, C., and De Flora, A. (1996) *FEBS Lett.* **396**, 327–332
 18. Zocchi, E., Usai, C., Guida, L., Franco, L., Bruzzone, S., Passalacqua, M., and De Flora, A. (1999) *FASEB J.* **13**, 273–283
 19. De Flora, A., Franco, L., Guida, L., Bruzzone, S., Usai, C., and Zocchi, E. (2000) *Chem. Immunol.* **75**, 79–98
 20. Bruzzone, S., Guida, L., Zocchi, E., Franco, L., and De Flora, A. (2001) *FASEB J.* **15**, 10–12
 21. Franco, L., Guida, L., Bruzzone, S., Zocchi, E., Usai, C., and De Flora, A. (1998) *FASEB J.* **12**, 1507–1520
 22. Franco, L., Zocchi, E., Usai, C., Guida, L., Bruzzone, S., Costa, A., and De Flora, A. (2001) *J. Biol. Chem.* **276**, 21642–21648
 23. Podestà, M., Zocchi, E., Pitto, A., Usai, C., Franco, L., Bruzzone, S., Guida, L., Bacigalupo, A., Scadden, D. T., Walseth, T. F., De Flora, A., and Daga, A. (2000) *FASEB J.* **14**, 680–690
 24. Nagy, J. I., Li, W. E. I., Roy, C., Doble, B. W., Gilchrist, J. S., Kardami, E., and Hertzberg, E. L. (1997) *Exp. Cell Res.* **236**, 127–136
 25. Laemmli, U. K. (1970) *Nature* **227**, 680–685
 26. Towbin, H., Staehelin, T., and Gordon, J. (1979) *Proc. Natl. Acad. Sci. U. S. A.* **76**, 4350–4354
 27. Bradford, M. M. (1976) *Anal. Biochem.* **72**, 248–252
 28. Chomczynski, P., and Sacchi, N. (1987) *Anal. Biochem.* **162**, 156–159
 29. Tamaoki, T., Nomoto, H., Takahashi, I., Kato, Y., Morimoto, M., and Tomita, F. (1986) *Biochem. Biophys. Res. Commun.* **135**, 397–402
 30. Nakanishi, S., Matsuda, Y., Iwahashi, K., and Kase, H. (1986) *J. Antibiot.* **39**, 1066–1071
 31. Toullec, I., Pianetti, P., Coste, H., Bellevergue, P., Grand-Perret, T., Ajakane, M., Baudet, V., Boissin, P., Boursier, E., Loriolle, F., Duhamel, L., Charon, D., and Kirilovsky, J. (1991) *J. Biol. Chem.* **266**, 17771–17781
 32. Davis, P. D., Elliott, L. H., Harris, W., Hill, C. H., Hurst, S. A., Keech, E., Kumar, M. K., Lawton, G., Nixon, J. S., and Wilkinson, S. E. (1992) *J. Med. Chem.* **35**, 994–1001
 33. Eichholtz, T., de Bont, D. B. A., de Widt, J., Liskamp, R. M. J., and Ploegh, H. L. (1993) *J. Biol. Chem.* **268**, 1982–1986
 34. Bialojan, C., and Takai, A. (1988) *Biochem. J.* **256**, 283–290
 35. Bruzzone, R., White, T. W., and Paul, D. L. (1996) *Eur. J. Biochem.* **238**, 1–27
 36. Lampe, P. D., and Lau, A. F. (2000) *Arch. Biochem. Biophys.* **384**, 205–215
 37. Walseth, T. F., and Lee, H. C. (1993) *Biochim. Biophys. Acta* **1178**, 235–242
 38. Brisette, J. L., Kumar, N. M., Gilula, N. B., and Dotto, G. P. (1991) *Mol. Cell. Biol.* **11**, 5364–5371
 39. Reynhout, J. K., Lampe, P. D., and Johnson, R. G. (1992) *Exp. Cell Res.* **198**, 337–342
 40. Franco, L., Bruzzone, S., Song, P., Guida, L., Zocchi, E., Walseth, T. F., Crimi, E., Usai, C., De Flora, A., and Brusasco, V. (2001) *Am. J. Physiol. Lung Cell Mol. Physiol.* **280**, L98–L106
 41. Zocchi, E., Podestà, M., Pitto, A., Usai, C., Bruzzone, S., Franco, L., Guida, L., Bacigalupo, A., and De Flora, A. (2001) *FASEB J.* **15**, 1610–1612
 42. Verderio, C., Bruzzone, S., Zocchi, E., Fedele, E., Schenk, U., De Flora, A., and Matteoli, M. (2001) *J. Neurochem.* **78**, 1–13
 43. Nicotera, P., and Orrenius, S. (1998) *Cell Calcium* **23**, 173–180
 44. Hertzberg, E. L., and Van Eldik, L. J. (1987) *Methods Enzymol.* **139**, 445–455
 45. Peracchia, C., Lazrak, A., and Peracchia, L. L. (1994) in *Handbook of Membrane Channels* (Peracchia, C., ed.) pp. 361–377, Academic Press, London
 46. Bernardi, P. (1999) *Physiol. Rev.* **79**, 1127–1155
 47. Di Lisa, F., Menabò, R., Canton, M., Barile, M., and Bernardi, P. (2001) *J. Biol. Chem.* **276**, 2571–2575
 48. Ziegler, M., Jorcke, D., and Schweiger, M. (1997) *Biochem. J.* **326**, 401–405
 49. Carafoli, E., Santella, L., Branca, D., and Brini, M. (2001) *Crit. Rev. Biochem. Mol. Biol.* **36**, 107–260
 50. Laing, J. G., Tadros, P. N., Westphale, E. M., and Beyer, E. C. (1997) *Exp. Cell Res.* **236**, 482–492